

...ance of this article, the  
...her or recipient acknowledges  
... U.S. Government's right to  
...tain a nonexclusive, royalty-free  
...license in and to any copyright  
...covering the article.

CHARACTERISTICS OF A LONG-PULSE (30-s), HIGH-POWER (4-MW)  
ION SOURCE FOR NEUTRAL BEAM INJECTION\*

M. M. Menon, G. C. Barber, S. K. Combs, W. K. Dagenhart, W. L. Gardner, H. H. Haselton,  
J. A. Moeller, N. S. Ponte, P. M. Ryan, D. E. Schechter, W. L. Stirling,  
C. C. Tsai, J. H. Wheaton, and R. E. Wright  
Oak Ridge National Laboratory, P.O. Box Y, Oak Ridge, TN 37831

Abstract

ORNL-DWG 82-2991 FED

A quasi-steady-state ion source has been developed for neutral beam injection applications. It is of the duoPIGatron type designed for delivering 50 A of hydrogen ions at 80 keV for 30-s-long pulses. Ion beams of 40 A at 75 keV were extracted for pulse lengths up to 30 s, maintaining excellent optical quality in the beam for the entire pulse duration. The design features and operational characteristics of the ion source are elaborated.

Introduction

Major magnetic confinement fusion experiments, such as the Tokamak Fusion Test Reactor (TFTR) and Mirror Fusion Test Facility (MFTF-B) in the United States, the Joint European Torus (JET) in Europe, and the JT-60 in Japan, are expected to use multisecond neutral beam injection at multimewatt power levels (10-30 MW).<sup>1</sup> Among these applications, the longest pulse length requirement is for the MFTF-B experiment, where ten injectors, each with a 30-s pulse duration, will be used. The Oak Ridge National Laboratory (ORNL) neutral beam program has been directed toward the development of such quasi-steady-state injectors. Apart from the long-pulse requirement, the MFTF-B application is characterized by high beam brightness (beam divergence of  $\leq 0.5^\circ$  at a deuterium current density of  $> 0.15 \text{ A}\cdot\text{cm}^{-2}$ ), high gas efficiency (a gas flow from each 50-A source of not more than  $10 \text{ torr}\cdot\text{L}\cdot\text{s}^{-1}$ ), high atomic species content (90%), and ultralow impurity content ( $10^{-5}$  part/injected  $\text{D}^0$ ). Because the last requirement is difficult to achieve in a conventional scheme, a magnetic beam purification scheme is being considered that will also lower the requirement on atomic species content to about 80%. A high degree of reliability (99%) is implied because of the simultaneous use of 10 long-pulse and 12 short-pulse (500-ms) injectors.

We describe the major features of an advanced positive ion source designed to provide a sufficient database for building a prototype ion source suitable for MFTF-B long-pulse injection.

Major Design Features

The Plasma Generator

The plasma generator, shown in Fig. 1, is of the ORNL duoPIGatron type<sup>2</sup> with several modifications to enable long-pulse operation. Unlike the short-pulse sources employed in the Princeton Large Torus (PLT) and Poloidal Divertor Experiment (PDX) injectors,<sup>3,4</sup> the long-pulse source utilizes two electron feeds, each incorporating an indirectly heated cathode. Each cathode has an emission area of about  $100 \text{ cm}^2$  on the inside surface of a paraboloid that is 5 cm in diameter at the open end (Fig. 2). The emitting shell is made by plasma spraying a mixture of 97.5% Mo, 2.0%  $\text{La}_2\text{O}_3$ , and 0.5% Pt by weight onto an aluminum mandrel to a thickness of 1.5 mm. Details of the fabrication and heat treatment of the cathode are given by Schechter and Tsai.<sup>5</sup> The emitting surface is radiatively heated by graphite heaters to about 1900 K with a heater

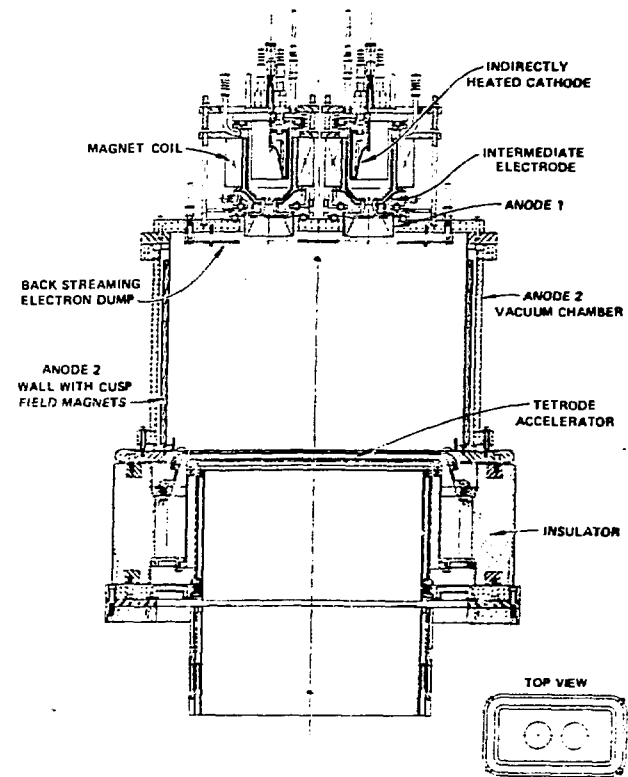


Fig. 1. The duoPIGatron ion source.

power of about 3.5 kW. Two of these cathodes are utilized in the plasma generator, which has a 28- by 60-cm anode cross section and a 30-cm-long anode chamber.

With regard to long-pulse operation, other modifications incorporated into the plasma generator are providing improved cooling and increasing the cusp field strength. Improved cooling is accomplished by active cooling of all the components exposed to high heat fluxes using electroformed water circuits. The cusp field magnets are mounted on electroformed copper liners located inside the vacuum chamber (see Fig. 1). This not only provides efficient cooling but also increases the magnetic field strength at the inner walls, since these walls are made thinner.

The Accelerator

The ion accelerator is designed using the two-dimensional (2-D) ion extraction code<sup>6</sup> developed at ORNL to minimize the aberration-limited beamlet divergence to  $0.26^\circ$  rms at a current density ( $D^+$ ) of  $0.15 \text{ A}\cdot\text{cm}^{-2}$ . The aperture shapes are illustrated in Fig. 3. The relatively thick (1-cm) ground electrode and the shape shown for the suppressor electrode minimize the backstreaming electron loading on the grids and the plasma generator.<sup>7</sup>

\* Research sponsored by the Office of Fusion Energy, U.S. Department of Energy, under Contract No. W-7405-eng-26 with the Union Carbide Corporation.

MASTER

DISTRIBUTION OF THIS DOCUMENT IS UNLIMITED

EAB

**DISCLAIMER**

This report was prepared as an account of work sponsored by an agency of the United States Government. Neither the United States Government nor any agency thereof, nor any of their employees, makes any warranty, express or implied, or assumes any legal liability or responsibility for the accuracy, completeness, or usefulness of any information, apparatus, product, or process disclosed, or represents that its use would not infringe privately owned rights. Reference herein to any specific commercial product, process, or service by trade name, trademark, manufacturer, or otherwise does not necessarily constitute or imply its endorsement, recommendation, or favoring by the United States Government or any agency thereof. The views and opinions of authors expressed herein do not necessarily state or reflect those of the United States Government or any agency thereof.

**NOTICE**

**PORTIONS OF THIS REPORT ARE ILLEGIBLE.**

**It has been reproduced from the best available copy to permit the broadest possible availability.**

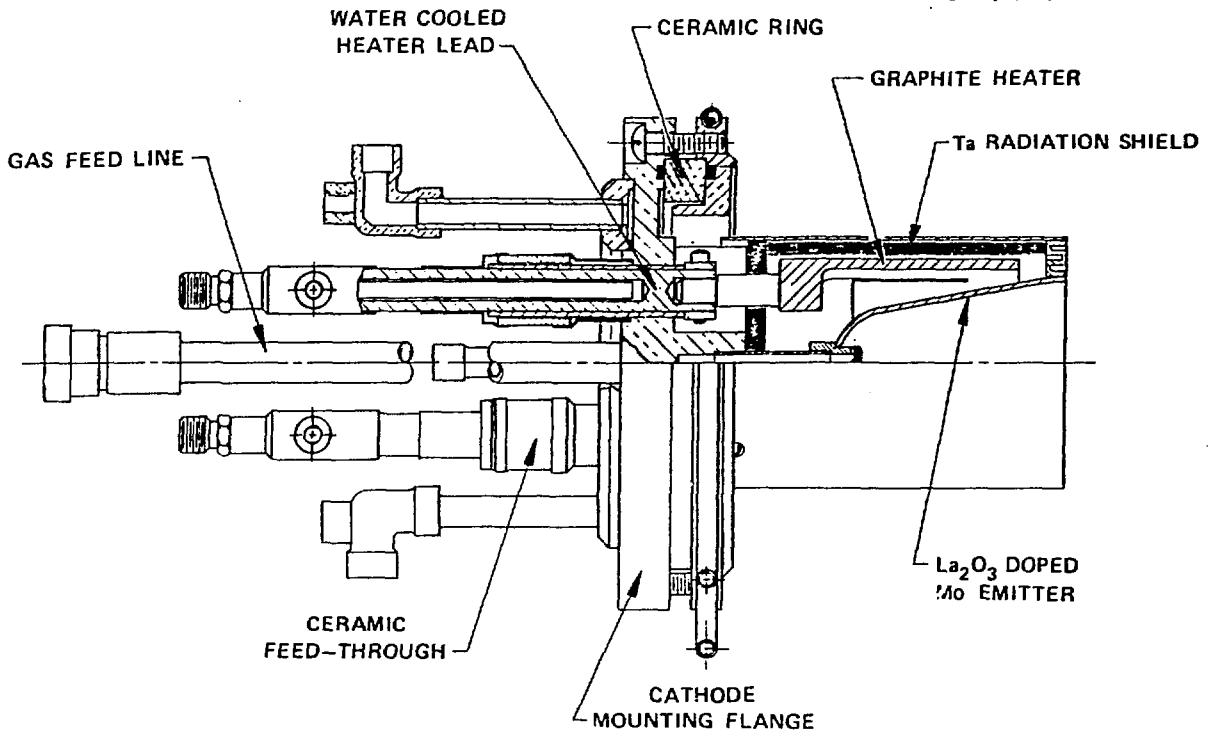


Fig. 2. Details of the indirectly heated cathode.

New techniques are used in the fabrication of the accelerator grids in order to improve the cooling efficiency while maximizing the grid transparency. Copper grids with a 13- by 43-cm active grid pattern and with serpentine cooling passages around each aperture are fabricated using electroforming techniques.

cathode, a single cathode was operated at a 500-A discharge level for thousands of 30-s-long pulses at a 30% duty cycle. The discharges were reliable, as illustrated by the chart in Fig. 6, which shows individual discharge pulses (vertical lines) as a function of operating hours.

Experimental Results

Beam Extraction

Arc Discharge

The plasma generator was operated at a 120-V, 1200-A arc discharge level for 35-s pulses (Fig. 4). The plasma uniformity was measured at a reduced pulse length (0.1 s) and the available uniform extraction surface was found to be 18 x 48 cm (Fig. 5). In an attempt to estimate the lifetime and reliability of the

Beam optics: The ion source was operated at beam energies up to 80 keV for short pulses (0.1-0.5 s) in order to characterize the beam optics. The beam profile was measured 420 cm downstream using a calorimetric probe. The beam optics is a function of the ratio of the electric fields in the first two gaps, and the numerical design is based on a field ratio between the second gap and the first gap of 2. Measurements

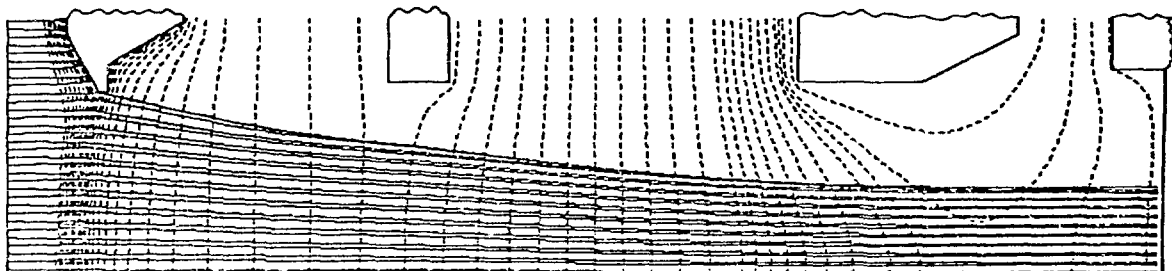
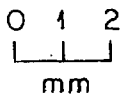


Fig. 3. Aperture geometry of the accelerator.

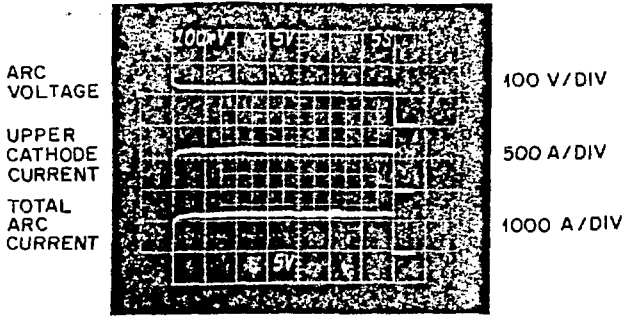


Fig. 4. Oscillogram of a 120-V, 1200-A, 35-s arc discharge.

were made at a field ratio of 1.8. Because the accelerator is focused on a point 950 cm downstream and because the profile measurement was made 420 cm downstream, the beamlet divergence was computed based on the best fit with the experimental data. A divergence angle of  $0.47^\circ$  rms at a field ratio of 1.8 was obtained, assuming Gaussian beamlets, perfect focusing, and constancy in perveance and field ratio during the entire pulse length.

Optimum perveance and tunability: Figure 7 shows a plot of power loading on different components as a function of perveance (perveance is defined as the ratio of the extracted current to the three-halves power of the acceleration voltage). The perveance is varied at constant acceleration voltage by varying the extracted current. The figure illustrates that the source can be tuned over a wide range of perveance. The optimum perveance that corresponds to the maximum power transmission to the target is about 1.8  $\mu$ perv. The grid loadings do not change appreciably with changes in perveance. It may be noted that these data are obtained using 100-ms pulses with a gas flow to the source significantly ( $\approx 50\%$ ) higher than that necessary for long-pulse operation. The rise time of the pulse, during which the beam is appreciably off its optimum perveance, is about 10 ms. These effects increase both the heat loadings on the grids and the beam transport losses. The power flow measured at a lower gas flow when the beam pulse length was 30 s appears later in the text (Fig. 10).

Atomic species: The species mix from the source was measured by scanning the ion deflection magnet current and noting the signal from a calorimetric probe. However, the technique was limited to low current densities since the deflection magnet was designed for a 50-keV beam. The beam pulse length was restricted to 0.06 s due to power density limitations on the ion dump. To complicate the measurement further, the gas flow from the source was not adequate to

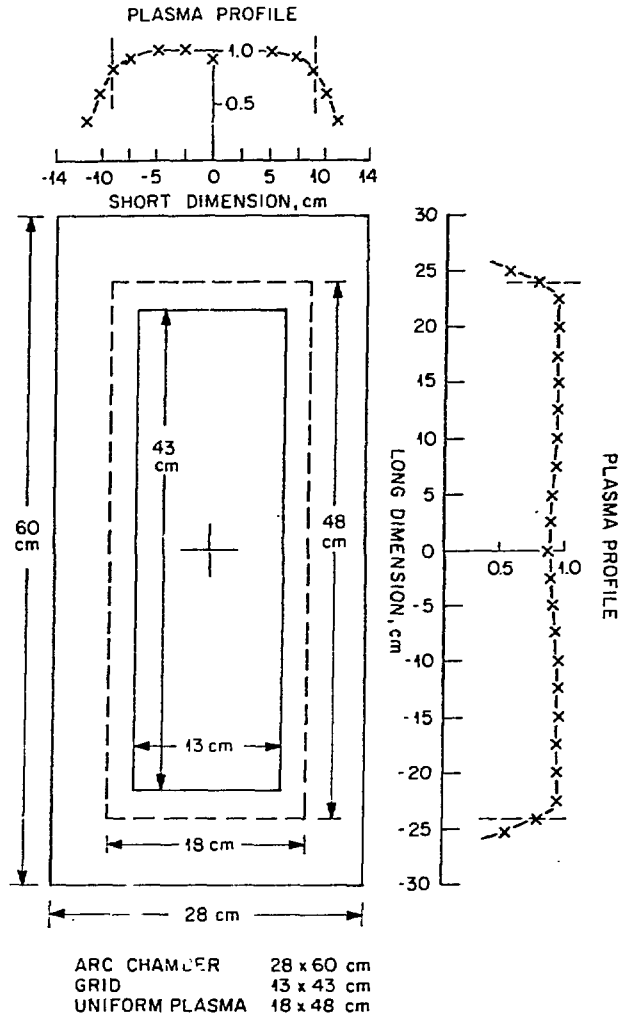


Fig. 5. Plasma density profile.

provide equilibrium neutralization. Additional gas, which had to be injected into the neutralizer, could enhance the half-energy component. Measurements of atomic species fraction at current densities up to  $0.076 \text{ A}\cdot\text{cm}^{-2}$  yielded values up to 69.5%. This should extrapolate to better than 80% at full current density, based on the familiar scaling of atomic fraction with current density observed with the PLT and PDX sources.<sup>6</sup> The actual atomic species content at the plasma extraction surface should be several percentage points above

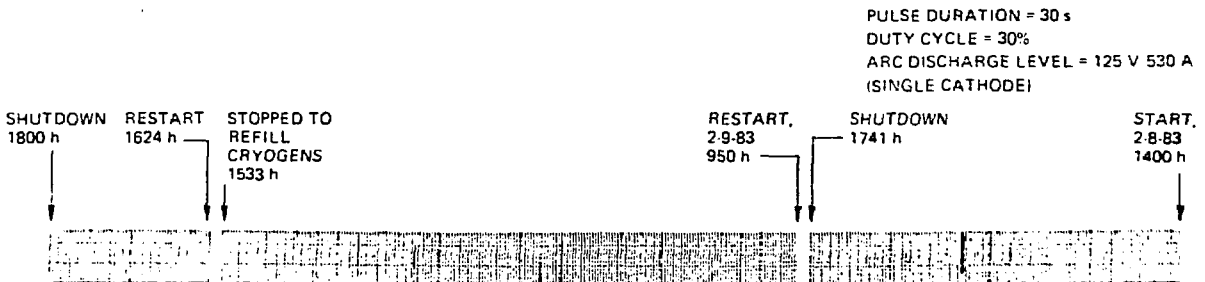


Fig. 6. Chart recorder output sample illustrating the cathode performance.

PULSE DURATION = 30 s  
 DUTY CYCLE = 30%  
 ARC DISCHARGE LEVEL = 125 V 530 A  
 (SINGLE CATHODE)

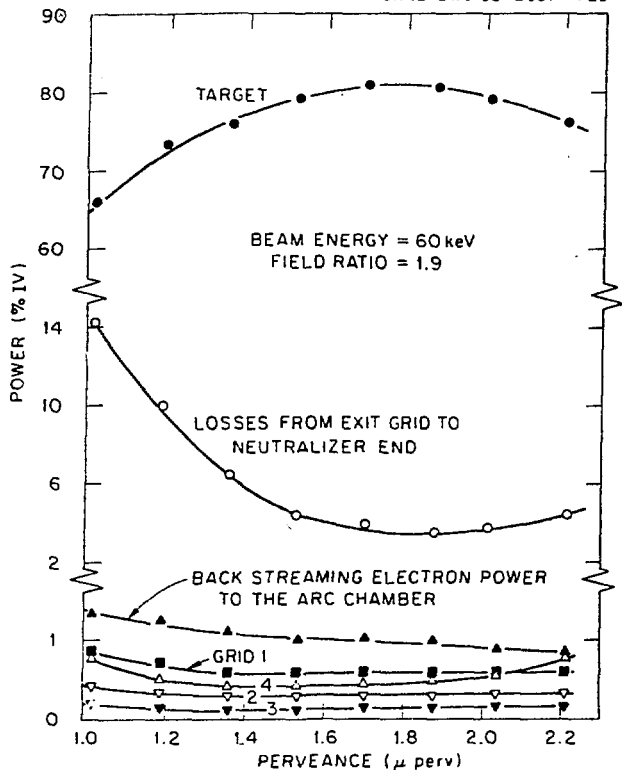


Fig. 7. Power dissipation vs perveance.

80% if the collisional processes in the accelerator region are taken into account.<sup>9</sup>

**Long-pulse operation:** The beam pulse length was gradually extended at 3 MW of extracted power (75 kV/40 A) to the full 30 s. During this exercise, the energy dissipated on different components of the ion source and the beam line was measured calorimetrically with the help of a computerized data acquisition system. A swirl tube calorimeter,<sup>10</sup> designed to intercept up to 5 MW of beam power at peak power densities of 25-30 kW/cm<sup>2</sup>, was employed to stop the beam. The energy dissipated in the swirl tube calorimeter was measured by noting the rise in the temperature of the water circulating through the calorimeter and the total water flow. However, this temperature signal was not compatible with the computerized data acquisition system. Therefore, in order to illustrate that the beam optics was not altered as the beam pulse length was extended, the energy dissipated on the beam scrapers located just before the calorimeter (at 520 cm downstream) is plotted along with the accelerator grid dissipation values in Fig. 8. It can be seen that with an increase in extracted energy (as the pulse length is increased), the dissipation on all the components increases linearly, establishing the integrity of the ion source design at energy levels approaching 100 MJ.

**Power flow:** For a 75-kV, 40-A beam pulse of 30-s duration (Fig. 9), the power flow along the beam line is shown in Fig. 10; the beam line itself is shown in Fig. 11. Note that more than 90% of the power from the ion source is transmitted to the target located 520 cm downstream. The gas flow to the source for this pulse was 10 torr·L·s<sup>-1</sup>, and this low gas flow and the excellent beam optics have resulted in the low grid loadings and beam transport losses shown in Fig. 10.

The power flow pattern confirms not only that the ion beam is of excellent optical quality but also that this optical quality is maintained throughout the quasi-steady-state beam operation.

Conclusions

A quasi-steady-state ion source has been developed and the operating characteristics determined. The ion source was demonstrated to be suitable for neutral injection applications involving beam pulses up to 30 s in duration at power levels up to 3 MW.

Acknowledgments

The authors are indebted to C. W. Blue, S. C. Forrester, F. Sluss, D. O. Sparks, and P. H. Hayes for their help.

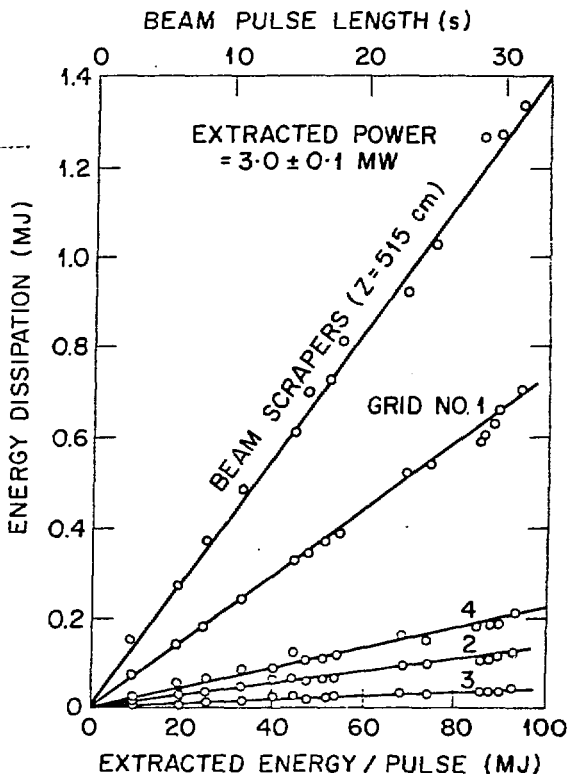


Fig. 8. Energy dissipation vs beam pulse length.

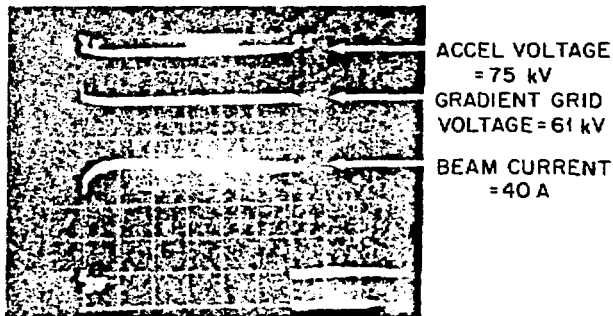


Fig. 9. Oscilloscope image of a 75-kV, 40-A beam pulse of 30-s duration.

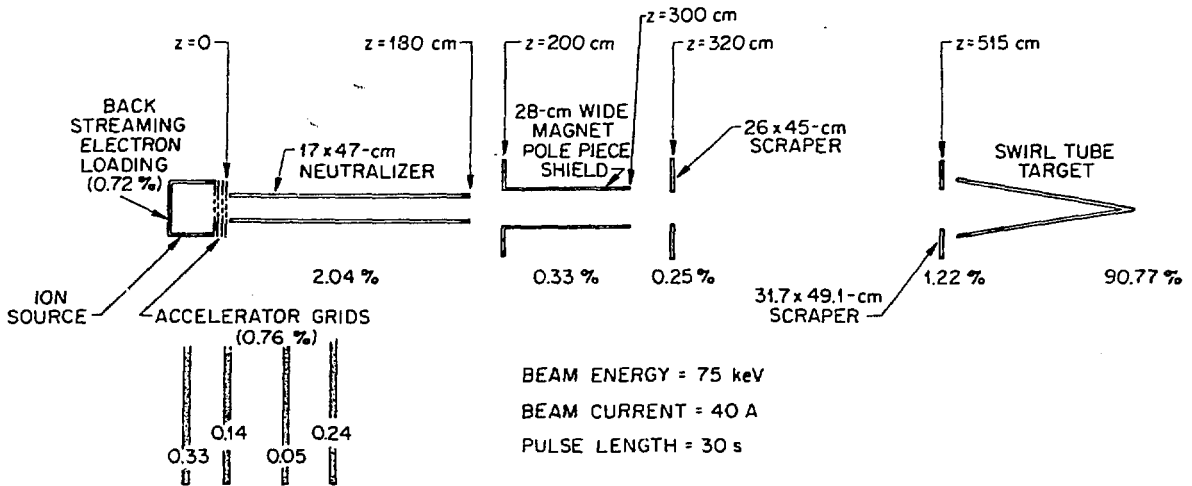


Fig. 10. Power flow along the beam for a 3-MW, 30-s pulse.

References

- [1] M. M. Menon, "The technology of neutral beam injection based on positive ion sources," *Nucl. Technol./Fusion*, vol. 4, pp. 625-631, Sept. 1983.
- [2] C. C. Tsai, W. L. Stirling, and P. M. Ryan, "Plasma studies on a duoPIGatron ion source," *Rev. Sci. Instrum.*, vol. 48, pp. 651-655, June 1977.
- [3] W. L. Stirling et al., "Properties of an intense 40-kV neutral beam injector," *Rev. Sci. Instrum.*, vol. 50, pp. 523-527, May 1979.
- [4] W. L. Gardner et al., "Properties of an intense 50-kV neutral beam injection system," *Rev. Sci. Instrum.*, vol. 53, pp. 424-431, April 1982.
- [5] D. E. Schechter and C. C. Tsai, "Indirectly heated cathode and duoplasmatron type electron feeds for positive ion sources," in *Proceedings of the 9th Symposium on Engineering Problems of Fusion Research*, 1981, vol. 2, pp. 1515-1518.
- [6] J. H. Whealton, E. F. Jaeger, and J. C. Whitson, "Optics of Ion Beams of Arbitrary Perveance Extracted from a Plasma," *J. Comput. Phys.*, vol. 27, pp. 32-41 (1978).
- [7] J. H. Whealton, "Primary ion tetrode optics for high transparency multi-beamlet neutral injectors," *J. Appl. Phys.*, vol. 53, pp. 2811-2817 (1982).
- [8] C. C. Tsai et al., "Determination of species yield of ion sources used for intense neutral beam injectors," *J. Nucl. Mater.*, vol. 111 & 112, pp. 153-158, 1982.
- [9] C. C. Tsai, "Energy straggling in an ion accelerator," in *Proceedings of the 3rd Neutral Beam Heating Workshop (CONF-8110118)*, 1981, pp. 433-442.
- [10] S. K. Combs et al., "Development of a high-heat-flux target for multimegawatt, multisecond neutral beams at ORNL," this conference.

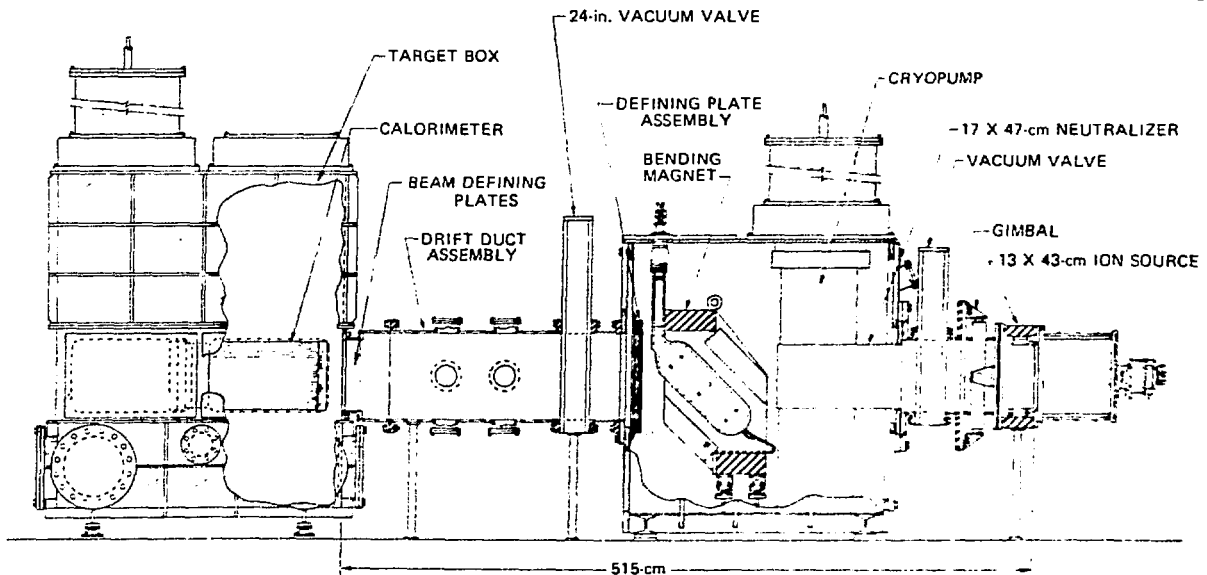


Fig. 11. The geometry of the beam line.